Auger-pumped short-wavelength lasers in xenon and krypton

H. C. Kapteyn and R. W. Falcone
Department of Physics, University of California, Berkeley, Berkeley, California 94720
(Received 11 September 1987)

We report studies of new short-wavelength lasers in xenon at 108.9 nm and krypton at 90.7 nm. The lasers are pumped by photoionization of inner-shell electrons followed by Auger decay into excited states. Experiments include measurement of gain and the lifetimes and quenching of the lasing states, the use of a mirror for multipass gain, and studies of the output pulse duration. Numerical simulations which predict gain and the time evolution of the laser output are compared with experiment.

The first demonstration of a short-wavelength laser pumped by Auger decay following photoionization was recently reported by the authors.[1] In this experiment, soft x rays emitted from a laser-produced plasma ionize inner-shell $4d$ electrons in neutral xenon gas. The resulting highly excited Xe^+ atoms rapidly undergo Auger decay to various excited states of Xe^{2+}. The relative Auger decay rates and level degeneracies are such that a population inversion is created between Xe^{2+} $5s^0 5p^6\,{}^1S_0$ and $5s^1 5p^5\,{}^1P_1$, and laser gain is observed at the transition wavelength of 108.9 nm. The analogous transition in krypton, Kr^{2+} $4s^0 4p^6\,{}^1S_0$ to $4s^1 4p^5\,{}^1P_1$, is similarly inverted and gain is reported here for the first time at the transition wavelength of 90.7 nm. We also present data on the lifetimes and quenching of these states, describe experiments in xenon in which multipass gain is observed, and describe a model which predicts gain and output pulse duration. In previous work[2] we reported branching ratios for Auger decay in the xenon system.

Duguay and Rentzepis[3] first proposed making short-wavelength lasers by photoionizing inner-shell electrons in atoms. The production of population inversions by selective Auger decay following inner-shell photoionization was later suggested by McGuire.[4] Several considerations make this scheme a potentially efficient way of producing short-wavelength lasers. First, a high-energy pulsed laser can be efficiently converted to intense, incoherent x rays by focusing it onto a solid target and thus creating a hot plasma.[5] This laser produced plasma radiates x rays which ionize adjacent gas atoms. Second, inner-shell photoionization cross sections and Auger branching ratios can be favorable for producing excited-state populations.[6] For example, laser-produced plasma radiation near 100 eV, which results from focused laser intensities of about 10^{12} W/cm^2 on metal targets, is well matched to the broad $4d$-electron ionization cross section in xenon.[7] Considering the typical conversion efficiency of laser energy to plasma radiation and typical Auger decay rates, we estimate that the potential conversion of pump laser energy to short-wavelength laser energy can exceed 10^{-4}. Recent work[8] at Standford University, in which gain in the xenon laser was saturated in a traveling-wave pump geometry, yielded pulses with energy greater than 20 μJ at 108.9 nm and a conversion efficiency exceeding 5×10^{-6}. Photoionization and Auger pumped laser schemes have advantages over other recently developed short-wavelength laser schemes[9,10] which require high particle densities for collisional or recombination pumping. These advantages include reduced refractive-index gradients in the lasing medium and a lack of kinetics which makes it possible to predict gain using simple numerical models, provided that atomic parameters such as photoionization cross sections, Auger decay rates, excited-state lifetimes, and gain cross sections are known.

The experimental apparatus used to demonstrate gain is shown in Fig. 1 (a more complete description is found in Ref. 1). Briefly, a Nd-doped glass laser pulse (40–70 J, 0.1–1 nsec) is focused onto a tantalum target to form a thin, 9-cm-long soft-x-ray source. Radiation from the plasma ionizes xenon or krypton gas in a 3 mm$\times$3mm$\times$9 cm channel opposite the plasma and 1–2 cm away from it. The channel is covered with a 150-nm-thick parylene filter which acts to confine the active region since it is a transparent to the pump soft x rays but is opaque to the short-wavelength laser radiation. The actual length of the gain region is varied by shadowing portions of the channel from the pumping radiation; emission from gas in the channel is expected to increase nonlinearly with pumped length if there is laser gain. The photodetector is a specially designed soft-x-ray streak camera with a microchannel plate photocathode.[11] The camera views the gas in the channel through a vacuum spectrometer. The system has a spectral resolution of 1.5 nm, a time resolution of 200 psec, and is sensitive to single photons. Data are recorded on calibrated film which is later digitized by an optical scanner for computer analysis.

Gain is observed at both the Xe^{2+} 108.9-nm transition, as seen in Fig. 2, and at the Kr^{2+} 90.7-nm transition, as seen in Fig. 3. The data were fitted by a spectrally integrated brightness function (shown by the solid lines) generated by consideration of narrow angular and spectrally unresolved emission from an inhomogeneously broadened line source with uniform gain along its length.[1] The fit yields the line center gain coefficient.

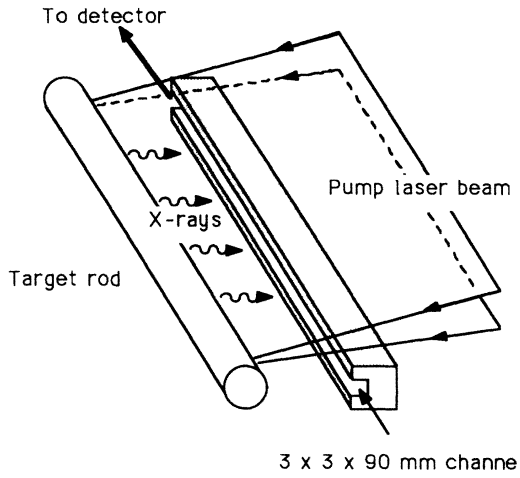

FIG. 1. Gain measurement apparatus showing the pump laser focused to a line on the target rod and the emission of soft x rays from the resulting plasma. The channel confines the observed region of the photoionized gas.

The xenon data were taken with 55 J of laser pump energy in a 1-nsec pulse and yield a gain coefficient of 0.8 cm^{-1}. Krypton data were taken with two different pump energies at a pulse length of 0.5 nsec. The indicated curve (*a*) is a fit to data taken with 50 J of pump energy, yielding a gain coefficient of 0.5 cm^{-1} and curve (*b*) is a fit to data taken with 38 J of pump energy, yielding a gain coefficient of 0.7 cm^{-1}. Fits are made to peak emission intensity; temporally integrated intensity data yield similar gain coefficients.

For the xenon experiments, the vacuum spectrometer is separated from the gas-filled target chamber by a 1-mm-thick lithium fluoride window. In the case of krypton, lithium fluoride is opaque to the emission wavelength. Therefore, a capillary array window (50-μm holes, 2-mm-thick, 50%-clear aperture) is used in a differential pumping geometry.[12] The capillary array separates the gas-filled target cell from an intermediate chamber pumped by a sorption pump. A 500 $\mu m \times 5$ mm entrance slit separates the intermediate chamber from the spectrometer, which is pumped by a turbomolecular

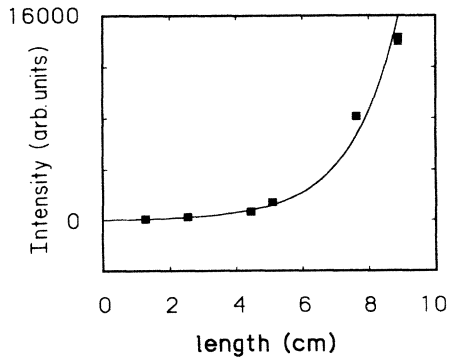

FIG. 2. Intensity as a function of pumped length for xenon emission at 108.9 nm. The solid line indicates the fit to the data for a gain coefficient of 0.8 cm^{-1}.

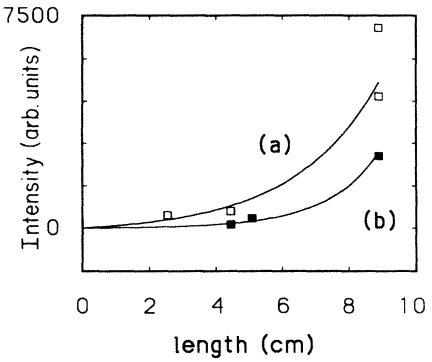

FIG. 3. Intensity as a function of length for krypton emission at 90.7 nm. Curve (*a*) indicates a fit to data taken with a pump enery of 50 J yielding a gain coefficient of 0.5 cm^{-1}. Curve (*b*) indicates a fit to data taken at a pump energy of 38 J yielding a gain of 0.7 cm^{-1}.

pump. A pressure of several torr can be maintained in the target cell, while maintaining a pressure in the vacuum spectrometer and at the streak camera detector of less than 5×10^{-5} torr. The capillary array is placed within 5 mm of the excited gas region so that photons with energy above the gas ionization potential can also be detected without significant loss.

Enriched isotopic xenon (80% $^{136}_{54}Xe$) is used to minimize the effects of isotope and hyperfine splitting which act to lower the gain; measured gain is about a factor of 2 smaller with the naturally occurring xenon isotopic mixture.[1] For krypton, the natural isotope mix contains 88% even-even isotopes with no hyperfine splitting.

The time structure of the emission from xenon shows interesting behavior as a function of increasing output intensity. Using the 1-nsec pump laser pulse and at low output intensity, the emission pulse width varies from 600 to 1200 psec. As the intensity increases (with increasing pumped length) a double peak structure appears. The second peak is delayed by about 800 psec and has an intensity of $\frac{1}{2}$ to $\frac{1}{3}$ of the first peak. As the pumped length is increased further, the two peaks reduce in separation until at the highest intensities a single peak of about 450 psec full width at half maximum (FWHM) is observed. The second peak appears to be a result of the gain dynamics of the system and is discussed later. In krypton, using a 500-psec pump pulse, all data show single pulses with a duration near the resolution limit of the detector.

In anticipation of construction of a resonator for this laser system, a reflector was used to enhance the output in a double pass geometry. The reflector is a lithium fluoride window which has a calculated surface reflectivity of about 10% at 108.9 nm.[13] In this experiment, the pump laser is focused to a line 9 cm long inside a 1-cm-deep by 3-mm-wide slot. Emission is observed from a region close to the plasma target. About 4 J of laser energy is necessary to show substantial gain on the 108.9-nm transition in this geometry. Gain is measured by alternately blocking and unblocking the mirror and varying the pumped length. As shown in Fig. 4, the mir-

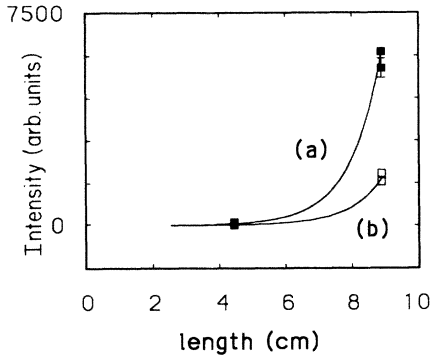

FIG. 4. Intensity as a function of length for xenon 108.9-nm emission. Curve (*a*) indicates a fit to data taken with a lithium fluoride reflector yielding a gain coefficient of 1.12 cm^{-1}. Curve (*b*) indicates a fit to data taken without the reflector and yields a gain of 1.09 cm^{-1}.

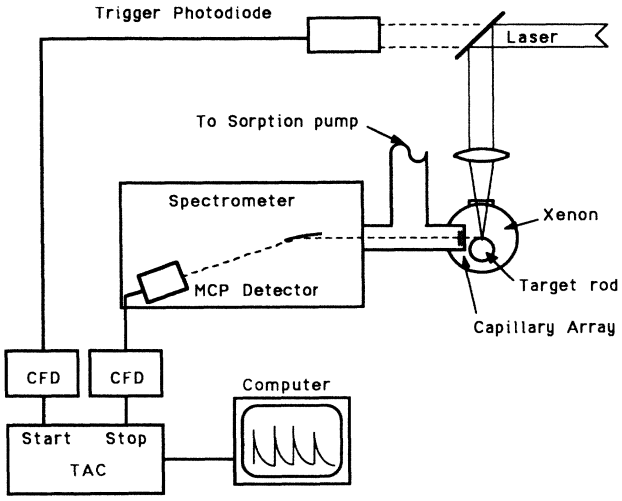

FIG. 5. Time-correlated photon counting apparatus.

ror enhances the output. Curve (*a*) is a fit to data with the reflector and curve (*b*) fits data without the reflector. The relatively small enhancement of output intensity in the multipass geometry, relative to the measured gain along the channel, may be explained by output saturation and the fact that gain is present in the system for a time comparable to or shorter than the optical round trip time in the channel.

In addition to studying these xenon and krypton transitions, we searched for other lines in the wavelength range of 50 to 100 nm in xenon, krypton, and argon. No other lasing transitions were found in either the channel configuration or in the slot configuration using a 30-J, 100-psec pump pulse.

The lifetimes of the upper and lower laser levels in xenon and krypton were measured using the technique of time-correlated photon counting[14] (TCPC) in conjunction with a high repetition rate laser-produced plasma x-ray source.[2,7] In TCPC, single photons are detected from the excited gas following repetitive impulsive excitation. The time interval between the excitation pulse and detection of a fluorescence photon is measured and a histogram of photon arrival times is constructed showing decay of the excited state. The apparatus is shown in Fig. 5 (a more complete description is found in Ref. 2). A *q*-switched, mode-locked Nd:YAG (yttrium aluminum garnet) laser is focused onto a rotating metal target rod. The output of the laser consists of bursts of about 20 pulses, with each pulse 100 psec long and separated by 10 nsec; the burst repetition rate is up to 500 Hz. Each pulse has an energy of up to 70 μJ and is focused by a 10-cm lens to a power density of about 10^{11} W/cm^2 on the target. Soft x rays from the resulting plasma excite gas surrounding the target, and fluorescence is detected by a microchannel plate photodetector at the exit slit of a vacuum monochromator. The target cell is separated from the spectrometer by a differential pumping system similar to that described previously. Since some of the fluorescence lines have energies above the ionization threshold, the capillary array window is placed within 1 cm of the excited gas region to minimize absorption. Although dust and debris from the repetitively pulsed plasma can clog the capillary array, this problem is mitigated by placing the gas inlet tube between the capillary array and the plasma, and by limiting the repetition rate of the laser to 50 Hz. The detection electronics consists of two constant fraction discriminators, one triggered by a photodiode looking at the laser output, and the other triggered by the photodetector after amplification. Discriminator outputs are connected to the start and stop inputs of a time-to-amplitude converter, whose output is fed to a computer. The data are then displayed and fit to an exponential decay function.

The time resolution of the system was estimated by observing the emission of a short-lived transition in Kr^{2+} at 55 nm. Figure 6(a) shows this measurement, summed over eight separate peaks spaced at 10-nsec intervals. The resulting pulse has a FWHM of less than 300 psec and a rise time of 125 psec. Figure 6(b) shows a measurement of the Kr^{2+} 90.7-nm laser transition at 1 torr pressure, along with the resulting fit to the lifetime. Upper state lifetimes in both xenon and krypton, as well as lower state lifetimes in krypton, were determined in this

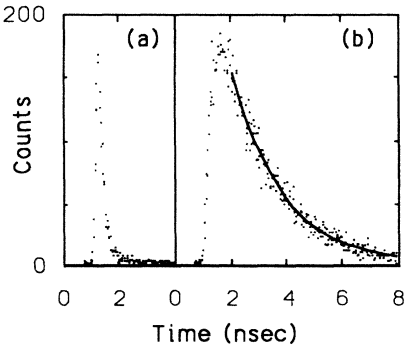

FIG. 6. Time-correlated photon counting data. (a) shows the time response of the system and (b) shows the decay of the krypton 90.7-nm transition at 1 torr pressure, with a fitted decay time of 1.84 nsec.

manner. However, the decay of the lower level of the Xe laser is complicated by cascade from the upper level on a time scale comparable to the 10-nsec pulse separation. This makes fitting the lower level lifetime difficult, so the laser system was modified to select a single pulse from the q-switched burst using an electrooptic crystal. The laser and pulse selector are run at 250 Hz in order to maintain high data rates. Lower level decays are then fit in the time interval when the upper level decay is substantially complete. Although electronic noise from the high voltage pulse selector causes several percent modulation of the decay curve with a 1–3-nsec period, these fluctuations average out over the lifetime.

At gas pressure on the order of 1 torr there is measurable neutral gas collisional quenching of the excited ions. Therefore, data are taken at various pressures and the natural lifetime is extrapolated to zero pressure assuming a linear collisional quenching coefficient C (torr^{-1} sec^{-1}). Laser energy on target is also varied to check for radiative trapping effects.[2] Measured lifetimes and collisional quenching coefficients are shown in Table I. The upper level of the xenon laser system decays primarily on the 108.9-nm transition, while the lower level decays on four transitions at 84.0, 90.1, 91.5, and 98.1 nm. For krypton, the upper level decays primarily at 90.7 nm, while the lower level decays at 78.6 nm, with weaker decays at 70.5, 73.2, and 91.9 nm.[15] Xenon upper level decay data[2] were taken using a lithium fluoride window at pressures up to 6 torr. Krypton upper level data were taken with the differential pumping geometry at pressures up to 4 torr. For lower levels in both gases, where the photon energy is above the ionization potential, data were taken with the differential pumping geometry at pressures up to 1.5 torr.

Computer simulations were developed to model the systems. These simulations involve two types of calculations. The first is a simple, time-independent calculation assuming instantaneous pumping of the xenon gas by the plasma x rays. This yields cumulative electron and ion densities, as well as the net gain coefficient. The second simulation is time dependent and takes into account amplified spontaneous emission. This is done to predict the temporal behavior of the output and to relate predicted local gain coefficients to the experimentally measured gain of the system as determined by the gain curve fit.

In these simulations, we assume that the plasma spectrum resembles a blackbody emitter with a 30-eV temperature and that the conversion efficiency of input laser energy to soft-x-ray emission is 7%.[5] The pump spectrum is divided into 600 energy bins between 0 and 300 eV. By calculating absorption of this radiation in the parylene filter[16] and in the gas (using cross sections[17] for the $4d$, $5s$, and $5p$ electrons), the densities of inner-shell and outer-shell ionized atoms and thus the total electron density can be determined. Secondary electron production due to electron avalanche ionization also occurs on a time scale comparable to the pump laser duration; this is taken into account by calculating an upper limit to electron density using energy considerations. The line plasma source is divided into 200 point source sections and excited-state densities are then calculated as a function of distance from the source, assuming radiation is emitted into 2π steradians. The population inversion density is then calculated using relative Auger decay fractions[2,18] of 0.044 and 0.051 for decay of the $4d$ hole state into the upper and lower laser levels, respectively. The gain cross section is calculated using standard formulas assuming Doppler broadening.

Calculations for the xenon gain experiment using this time independent model predict an exponential gain coefficient of 1.5 cm^{-1} along the 9-cm channel. Maximum total transverse gain is $e^{0.5}$. The excited-state density along the slot is calculated to be constant to within 20% of the average value over 80% of the slot length, and the maximum electron density is predicted to be 1×10^{15} cm^{-3}. By omitting the parylene filter, the calculated gain increases to 2.2 cm^{-1} and the electron density increases to 2×10^{15} cm^{-3}.

Since the observed output pulse from the xenon is shorter than the pump pulse, the gain computed above is expected to be only a rough estimate of the actual measured gain. Thus we developed the time-dependent model to more accurately predict the gain observed, and also to enable us to understand the pulse width behavior of the system under varying conditions. In this model, three major approximations are made to simplify the implementation. First, the excited-state density of the system is assumed to be uniform over the entire slot. Second, the photon transit time through the slot is assumed to be small compared to the characteristic time of both the pump pulse and the output pulse. And third, superfluorescence effects[19] are ignored and the output is assumed to be determined solely by amplified spontaneous emission.

In the model, a probability distribution function is first generated for photons traversing a distance x in the channel before exciting the gain medium. This is done using a Monte Carlo simulation for each excited channel length

TABLE I. Lifetime data for xenon and krypton upper and lower laser levels. The wavelength, decay time, and collisional quenching coefficient are indicated.

	Transition	λ (nm)	τ (nsec)	C (torr sec)$^{-1}$
Xe upper	$5s^1 5p^5\,{}^1P_1 - 5s^0 5p^6\,{}^1S_0$	108.9	4.75±0.15	$2.8\pm0.2\times10^7$
Xe lower	$5s^2 5p^4\,{}^3P_0 - 5s^1 5p^5\,{}^1P_1$	90.2	20.5±2.0	$2.3\pm0.5\times10^7$
Kr upper	$4s^1 4p^5\,{}^1P_1 - 4s^0 4p^6\,{}^1S_0$	90.7	2.0±0.1	$3.4\pm0.6\times10^7$
Kr lower	$4s^2 4p^4\,{}^1D_2 - 4s^1 4p^5\,{}^1P_1$	78.6	4.5±0.3	$1.8\pm1.1\times10^7$

considered. The simulation also determines how many of the photons exit the channel in the solid angle of the detector. A time-dependent gain simulation is then done using the Monte Carlo–generated distribution functions. In this model amplified spontaneous emission decreases the inversion by transferring population to the lower laser level, which we assume does not decay. Atoms are assumed to radiate equally in all directions but amplification is angle dependent due to the aspect ratio of the gain channel. Using the model, the expected output intensity and the pulse width are determined. For a given pumping flux these output parameters are calculated for a $\frac{1}{4}$-, $\frac{1}{2}$-, $\frac{3}{4}$-, and full-length slot. The resulting output intensity data from the model are then fit to the same gain function used to analyze the experimental data as described above. Given a pump pulse length of 1 nsec and a total pump flux identical to that determined in the time-independent model, the time-dependent model predicts a fitted gain parameter of 0.95 cm^{-1}. This is in reasonable agreement with the measured 0.8-cm^{-1} gain. The model predicts also that this measured gain is close to saturation in the system.

According to the results of the simulation, the output pulse length should shorten with increasing observed intensity, until saturation when the output pulse has a width of 430 psec. At higher output intensities the pulse width increases. Figure 7 shows the experimental pulse width data as a function of intensity; fits to the time-independent model data are shown as solid lines. Curve (*a*) is the model result assuming the predicted pump flux which, as discussed above, yields a reasonable fit to the intensity versus length data. However, the pulse length in this simulation is longer and increases more rapidly with decreasing length than the experimental data. By assuming only a 30% higher pump flux and thus higher gain, we obtain better agreement with the data as shown by curve (*b*). Thus the behavior of the amplitude and pulse length of the output can be reasonably accurately simulated using this model with only one empirical parameter. Although the model involves many simplifying assumptions (for example, it ignores possible electron quenching of the laser level) we conclude that amplified spontaneous emission is the dominant process determining the behavior of the xenon laser system.

The model does not, however, predict the observed double pulse output. Possible explanations include nonuniformities in the pumped gain region such as spatially dependent depletion rates, transit time effects, electron quenching of the lower level, or coherent effects.

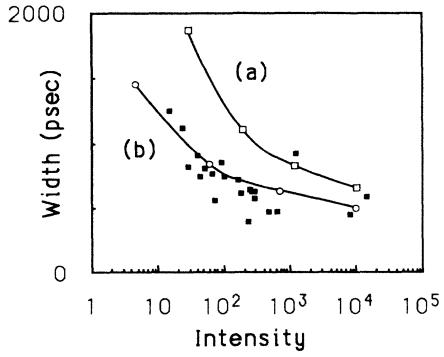

FIG. 7. Pulse length as a function of output intensity for the xenon transition at 108.9 nm. The solid lines are the model predictions. Curve (*b*) assumes a 30% higher gain than curve (*a*).

Superfluorescent behavior might be expected in our high gain, narrow linewidth gain medium since the coherence time (which is on the order of the upper state lifetime) is longer than the optical transit time through the gain region. Double output pulses have been predicted and observed in superfluorescent systems.[19]

In conclusion, we demonstrated gain in two new short-wavelength laser systems pumped by inner-shell photoionization and Auger decay. We measured lifetimes and quenching of the important states, and demonstrated the use of a reflector for multipass amplification. Time-dependent simulations were used to model the temporal behavior of these systems and to demonstrate that the primary effect determining the output pulse length of the laser under our pumping conditions is amplified emission. Further studies could include development of short cavity length or synchronously pumped resonators for these lasers, and the extension of the Auger pumping scheme to shorter wavelengths.

The authors thank Margaret Murnane, Richard Lee, Mau Chen, Jim Scofield, Geoffrey Kolbe, and Gary Power for their assistance. This work was supported by the National Science Foundation, the Institutional Research and Development Program at Lawrence Livermore National Laboratory, the Center for X-Ray Optics at Lawrence Berkeley Laboratory, AT&T Bell Laboratories, Schlumberger Doll Research, Amoco, and Newport Corporation.

[1]H. C. Kapteyn, R. W. Lee, and R. W. Falcone, Phys. Rev. Lett. **57**, 2939 (1986).

[2]H. C. Kapetyn, M. M. Murnane, and R. W. Falcone, Opt. Lett. **12**, 663 (1987).

[3]M. A. Duguay and P. M. Rentzepis, Appl. Phys. Lett. **10**, 350 (1967).

[4]E. J. McGuire, Phys. Rev. Lett. **35**, 844 (1975).

[5]R. G. Caro, J. C. Wang, R. W. Falcone, J. F. Young, and S. E. Harris, Appl. Phys. Lett. **42**, 9 (1983); R. G. Caro, J. C. Wang, J. F. Young, and S. E. Harris, Phys. Rev. A **30**, 1407 (1984).

[6]A. J. Mendelsohn and S. E. Harris, Opt. Lett. **10**, 128 (1985).

[7]H. C. Kapteyn, M. M. Murnane, R. W. Falcone, G. Kolbe, and R. W. Lee, in *Multilayer Structures and Laboratory X-Ray Laser Research,* Proceedings of the International Society for Optical Engineering, Bellingham, WA, 1987, edited by N. M. Ceglio and P. Dhez (SPIE, Bellingham, 1987), Vol. 688, p. 54.

[8]G.-Y. Yin, C. P. Barty, D. A. King, D. J. Walker, S. E. Harris,

and J. F. Young, Opt. Lett. **12**, 331 (1987); M. H. Sher, J. J. Macklin, J. F. Young, and S. E. Harris, Opt. Lett. **12**, 89 (1987).

[9]D. L. Mathews, P. L. Hagelstein, M. D. Rosen, M. J. Eckart, N. M. Ceglio, A. U. Hazi, H. Medecki, B. J. MacGowan, J. E. Trebes, B. L. Whitten, E. M. Campbell, C. W. Hatcher, A. M. Hawryluk, R. L. Kauffman, L. D. Pleasance, G. Rambach, J. H. Scofield, G. Stone, and T. A. Weaver, Phys. Rev. Lett. **54**, 110 (1985).

[10]S. Suckewer, C. H. Skinner, H. Milchberg, C. Keane, and D. Voorhees, Phys. Rev. Lett. **55**, 1753 (1985).

[11]H. C. Kapteyn, W. W. Craig, G. D. Power, J. Schachter, and R. W. Falcone (unpublished).

[12]T. B. Lucatorto, T. J. McIlrath, and J. R. Roberts, Appl. Opt. **18**, 2505 (1979).

[13]D. M. Roessler and W. C. Walker, J. Opt. Soc. Amer. **57**, 835 (1967).

[14]D. V. O'Connor and D. Phillips, *Time-Correlated Single Photon Counting* (Academic, London, 1984).

[15]All wavelengths are taken from the following sources: A. Striganov and N. Sventitskii, *Tables of Spectral Lines of Neutral and Ionized Atoms* (IFI/Plenum, New York, 1968); J. J. Hansen, F. G. Meijer, M. Outred, W. Persson, and H. O. Di Rocco, Phys. Scr. **27**, 254 (1983); M. Agentoft, T. Andersen, J. E. Hansen, W. Persson, and S.-G. Pettersson, *ibid.* **29**, 57 (1984).

[16]R. Stern and F. Paresce, J. Opt. Soc. Am. **65**, 1515 (1975).

[17]J. Berkowitz, *Photoabsorption, Photoionization and Photoelectron Spectroscopy* (Academic, New York, 1979).

[18]L. O. Werme, T. Bergmark, and K. Sigbahn, Phys. Scr. **6**, 141 (1972); S. Southworth, U. Becker, C. Truesdale, P. Kobrin, D. Lindle, S. Owaki, and D. Shirley, Phys. Rev. A **28**, 261 (1983); H. Aksela, S. Aksela, and H. Pulkkinen, Phys. Rev. A **30**, 865 (1984).

[19]M. F. H. Schuurmans, Q. H. F. Vrehen, and D. Polder, Ad. At. Mol. Phys. **17**, 167 (1981).

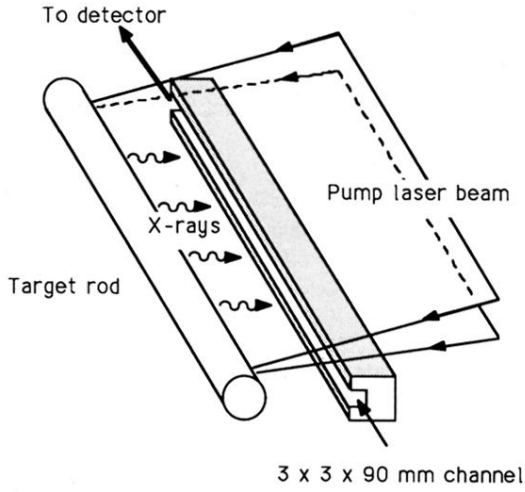

FIG. 1. Gain measurement apparatus showing the pump laser focused to a line on the target rod and the emission of soft x rays from the resulting plasma. The channel confines the observed region of the photoionized gas.